

# Impulsively Fast Magnetic Reconnection in Solar Flares and Coronal Mass Ejections and in Laboratory Plasma Merging Experiments

C. Z. Cheng<sup>1</sup>, Y. Ono<sup>2</sup>, Y. Hayashi<sup>2</sup>, Y. H. Yang<sup>3</sup>, G. S. Choe<sup>4</sup>

<sup>1</sup> Plasma and Space Science Center, National Cheng Kung University, Taiwan

<sup>2</sup> Department of Advanced Energy, University of Tokyo, Japan

<sup>3</sup> Institute of Space Science, National Central University, Taiwan

<sup>4</sup> Department of Astronomy and Space Sciences, Kyung Hee University, Korea

## Abstract

A mechanism of impulsively fast magnetic reconnection associated with acceleration of flux rope motion is presented. As the flux rope moves away from the reconnecting current sheet, its velocity is accelerated and then reaches to a constant value or decreases. The reconnection rate is peak concurrently with the maximum acceleration. In solar flares and coronal mass ejections, the model explained that the impulsive non-thermal hard X-ray emission occurred during the solar flare rising phase is correlated in time with the acceleration phase of coronal mass ejections. The model also predicts the peak reconnection electric field in the current sheet to be about 1 kV/m for X-class flares, which is later confirmed by the magnetic reconnection electric field estimation inferred from the observed two-ribbon expansion of solar flares. We also demonstrated for the first time in laboratory plasma merging experiments the correlation of the impulsively fast magnetic reconnection with the acceleration of plasmoid ejected from the current sheet using the TS-4 device of the Tokyo University. We conclude that the plasmoid/flux rope acceleration is a key mechanism for the impulsive enhancement of magnetic reconnection rate.

## 1. Impulsively Fast Magnetic Reconnection in Solar Flares and Coronal Mass Ejections

Magnetic reconnection is considered as the most important physical process in large scale energy release such as solar flares. Observations of solar flares and coronal mass ejections (CMEs) by the GOES, SOHO, YOHKOH, TRACE and RHESSI satellites and ground solar telescopes have greatly improved our understanding of the flare and CME dynamics and structure. Large flare events are typically observed first as a rapid rise in soft X-ray (SXR) emission observed by the GOES satellite, followed by simultaneous conjugate footpoint brightening in H $\alpha$ , UV and hard X-ray (HXR) and an ascending CME loop. The flare emission tends to have a cusp-shape SXR loop stretching across the magnetic neutral line that separates the regions of opposite polarity magnetic field in the photosphere to form arcade structure in the lower corona, and the footprints of the flare loops form a two-ribbon structure in the chromosphere. The outer flare loops have higher temperature. The height of the loop and the separation between the 2 ribbons increase with time. The most intense peak in the HXR (>25 keV) emission occurs at the time of maximum acceleration of the CME upward motion and is located at the outer parts of the ribbons. Besides the 2-ribbon structure, an HXR source is also occasionally observed at the apex of SXR loop.

An arcade magnetic field reconnection model has been proposed to explain the dynamics

and structure of the flare loops, the 2-ribbon emission, and the loop-top HXR source. When the magnetic field lines from different polarity region come into contact, magnetic reconnection occurs and the reconnection electric field (E-field) accelerate particles to high energies which stream along the newly reconnected field lines to hit the thick target plasma in the chromosphere to produce 2-ribbon emission. The plasma outflow from the current sheet will heat up the downstream plasma to produce SXR emission. As the reconnection process proceeds, the outer arcade field lines will come to reconnect and thus the footpoints of the newly reconnected field lines will expand outward, which indicates the expansion of the 2 ribbons away from the neutral line. Thus, by measuring the expansion of the 2 ribbons and the rate of the magnetic flux the ribbons sweep we can calculate the reconnection E-field at the reconnection X-line.

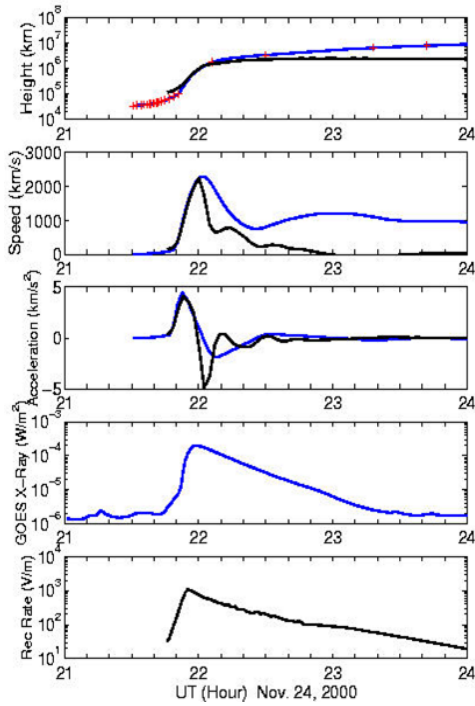


Fig. 1. Height, velocity and acceleration of CME and SXR emission light curve observed by GOES for the X1.8 flare-CME event on Nov. 24, 2000, and the model reconnection electric field at the X-line. The blues and red curves are observed values and the black curves are results of resistive MHD simulation

In particular, the CME upward motion is rapidly accelerated in the low corona during the rise phase of intense SXR flares. Figure 1 shows the CME upward motion, velocity and acceleration and the associated GOES SXR emission for a CME-X1.8 flare event (peak SXR emission of  $1.8 \times 10^{-4} \text{ W/m}^2$ ) observed on Nov. 24, 2000. Red points and Blues curves are observed values and black curves are results of resistive MHD simulation using anomalous resistivity. The HXR emission is impulsively released at  $\sim 21:53 \text{ UT}$  for  $\sim 2\text{-}3$  minutes during the SXR rise phase. By deploying resistive MHD simulation [1] with anomalous resistivity we were able to fit the observed CME motion curves and obtained the reconnection E-field at the reconnecting X-line, which is peaked at  $\sim 1 \text{ kV/m}$  at the time of maximum CME

As a result of the magnetic reconnection, a magnetic flux rope is formed above the X-line. The flux rope has helical magnetic field structure, and the plasma is confined inside to form a plasmoid. The plasmoid is observed above the loop-top HXR source in the H<sub>a</sub>/UV filament or SXR plasma ejecta in the low corona and as the CME in white light emission in the high corona and the interplanetary space. As the magnetic reconnection proceeds, the flux in the flux rope increases and the flux rope rises upward by  $\vec{j} \times \vec{B}$  force. The flux rope rising motion usually has 3 phases of rising speed: the lower rising speed phase corresponds to the pre-flare phase, the rising speed acceleration phase corresponds to the flare impulsive phase, and the long high speed phase (with weak acceleration or gradual deceleration) corresponds to the flare main phase.

Almost all CMEs are accompanied by large flares with the peak SXR emission intensity of  $\geq 10^{-5} \text{ W/m}^2$  observed by the GOES satellite, which suggests that there is a common physical mechanism underlying both flare and CME phenomena. The relationship between CME propagation and X-ray flare emission has been actively examined based on the combined observations.

acceleration. Thus, the resistive MHD model of the flare-CME event predicted that the peak reconnection E-field is  $\sim O(1 \text{ kV/m})$  for X-class flares [1]. The predicted peak reconnection E-field was later confirmed by many investigations of the E-field estimation using the observed magnetogram data and 2-ribbon expansion in H $\alpha$ , UV and HXR [e.g., 2-5].

## 2. Impulsive Magnetic Reconnection Process in Laboratory Plasma Merging Experiments

The impulsively fast magnetic reconnection has also been demonstrated for the first time in laboratory plasma merging experiments that the plasmoid (flux rope) dynamics is closely related to the impulsively fast magnetic reconnection. In particular, we show that the acceleration of plasmoid ejection velocity coincides with the impulsive enhancement of reconnection E-field (or reconnection rate) in the current sheet.

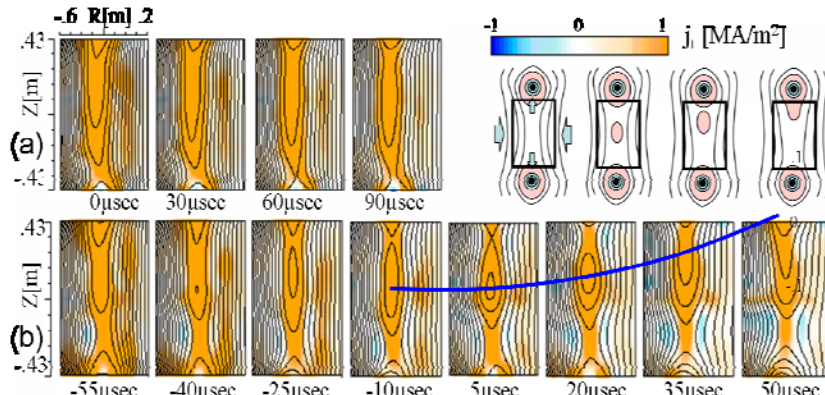


Fig. 2 Poloidal flux contours with toroidal current density  $j_t$  (red and blue colors) under high inflow condition.

The plasma merging experiments were performed by using the TS-4 device at University of Tokyo [6,7], which has a cylindrical vacuum vessel (length: 2 m, diameter: 1.7 m) with two poloidal field (PF) coils for poloidal flux injection and a central toroidal field (TF) coil for guide field  $B_t$

application in the toroidal direction. With the guide field  $B_t$  as high as five times of the reconnecting field  $B_p$ , two plasma toroids with  $R \approx 0.5\text{m}$  and  $R/a \approx 1.4$  formed around the PF coils were pulled out in the axial direction by swinging down the PF coil current [8-10]. The 1-m long current sheet with plasma parameters of  $T_i \approx T_e \approx 10\text{eV}$ ,  $n_e \approx 5 \times 10^{19} \text{ m}^{-3}$  and  $B_t \approx 1\text{kG}$  was produced in the axial direction between the two PF coils. The merging/reconnection process was controlled by the PF coil currents and the separation coil currents on the midplane [7]. Figure 2(a) shows the poloidal flux contours and the toroidal current density (in color) of slow reconnection of two merging plasma toroids which were slowly pulled out by the two PF coils [8-10]. We can identify the formation of a small plasmoid, but its position did not change for 100-150  $\mu\text{sec}$  due to the slow flux pileup rate.

Figure 2(b) shows the temporal evolution of poloidal flux contours for the case when a large plasmoid was ejected from the X-point area under the high inflow speed condition. The plasmoid was first formed around the X-point and grew in size from -40 to -10  $\mu\text{sec}$ , increasing its size from 10 cm to 20 cm. It was finally ejected in the axial (Z) direction from 0 to 50  $\mu\text{sec}$ , causing significant thinning of the current sheet down to 8 cm. Figure 3(a) shows the time evolution of the plasmoid central (O-point) position Z, its velocity  $V=dZ/dt$ , and its acceleration rate  $dV/dt$  for the case of Fig. 2(b). The plasmoid speed increased slowly from  $t = 0$  to 15  $\mu\text{sec}$  and then rapidly to 5km/sec from  $t = 15$  to 40  $\mu\text{sec}$ . Its acceleration  $dV/dt$

reached a peak value of  $\sim 20 \text{ km/s}^2$  at  $t \sim 25 \mu\text{sec}$  and then decreased after  $30 \mu\text{sec}$ . Figure 3(b) shows the evolution of reconnecting (toroidal) E-field  $E_t$  and the effective resistivity  $\eta = E_t/j_t$  of the current sheet at the X-point. The effective resistivity  $\eta$  includes all current sheet dissipations such as electron scattering effects by ions and various waves.

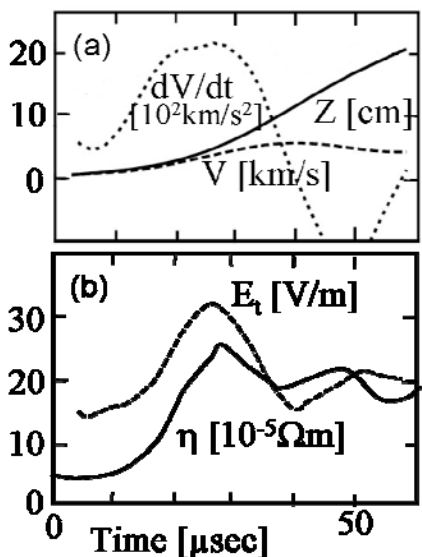


Fig. 3 Evolution of reconnection electric field  $E_t$ , position  $Z$ , velocity  $V$  and acceleration  $dV/dt$  of ejecting plasmoid under the high inflow condition.

It is noted that just like  $dV/dt$ , both the reconnecting E-field  $E_t$  and the effective resistivity  $\eta$  increased and reached their peak values when  $dV/dt$  is maximum at about  $t \sim 25 \mu\text{sec}$ , and then decreased before the plasmoid acceleration became negative after  $t \sim 40 \mu\text{sec}$ . This result indicates that the acceleration rate of plasmoid ejection velocity is strongly correlated with fast magnetic reconnection rate and effective resistivity of the current sheet. Although the externally-driven inflow compresses the current sheet, the acceleration of plasmoid ejection from the current sheet reduces significantly the thermal pressure inside the sheet and causes further thinning of the current sheet. The current sheet thinning and the reconnection E-field reached their maximum values simultaneously when the plasmoid acceleration reached its maximum. The thinning of current sheet enhances the current density and causes anomalous resistivity of the

current sheet and thus faster reconnection rate.

### 3. Summary

In conclusion, we have shown an impulsively fast magnetic reconnection mechanism by the acceleration of plasmoid/flux rope ejection for both solar flare-CME observations and laboratory plasma merging experiments. The reconnection rate correlates with the acceleration of the plasmoid/flux rope velocity, which suggests that the reconnection rate is controlled by the acceleration of plasmoid/flux rope ejection.

### References

- [1] C. Z. Cheng, Y. Ren, G. S. Choe and Y. J. Moon, *Astrophys. J.* 596, 1341 (2003).
- [2] J. Qiu, H. Wang, C. Z. Cheng and D. E. Gary, *Astrophys. J.* 604, 900 (2004).
- [3] Y. H. Yang, C. Z. Cheng, S. Krucker and M. S. Hsieh, *Astrophys. J.* 732, 15 (2011).
- [4] S. Krucker, M. D. Fivian and R. P. Lin, *Adv. Space Res.* 35, 1707 (2005).
- [5] C. Liu and H. Wang, *Astrophys. J.* 696, L27 (2009).
- [6] Y. Ono, M. Yamada, M. Katsurai, *Physics of Fluids B* 6, 3691 (1993).
- [7] Y. Ono, M. Inomoto, T. Okazaki and Y. Ueda, *Physics of Plasmas* 4, 1953 (1997).
- [8] Y. Ono, M. Inomoto, Y. Ueda and T. Matsuyama, *Science and Technology of Advanced Material*, 2, 473 (2001).
- [9] M. Yamada, H. Ji, S. Hsu, T. Carter, R. Kulsrud, Y. Ono and F. Perkins, *Phys. Rev. Lett.* 78, 3117 (1997).
- [10] M. Yamada, Y. Ren, H. Ji, J. Breslau, S. Gerhardt, R. Kulsrud and A. Kuritsyn, *Phys. Plasmas* 13, 052119 (2006).